Organic Process Research & Development **2011,** *15,* 104–111

Development of a Suitable Salt Form for a GPR40 Receptor Agonist

Henry Morrison,* Jonan Jona, Shawn D. Walker, Jacqueline C. S. Woo, Lan Li, and Jan Fang

Amgen Inc, One Amgen Center Drive, Thousand Oaks, California 91320, United States

Abstract:

AMG 837 (1) is a novel GPR40 agonist selected for clinical development for the treatment of type 2 diabetes. A lysine salt was initially identified as a development form. However, due to the poor crystallinity and severe hygroscopicity of this form, investigations on the free acid form of the drug substance and salt screening were conducted to identify an acceptable physical form for long-term development. A sodium and calcium salt were identified as potentially viable phases, and polymorph screening was conducted on both. The quality attributes of the salts were then compared to determine which phase would be preferred for development.

1. Introduction

AMG 837 (**1**) is a small molecule agonist of GPR40, a receptor highly expressed on pancreatic beta cells (Figure 1).[1,2] In multiple animal models of diabetes, activation of GPR40 results in insulin secretion and lowers blood glucose through amplification of intracellular calcium signaling.[3−8] Since GPR40-induced insulin secretion is glucose dependent, a potential reduced risk of hypoglycemia makes this target of particular interest in the search for novel treatments for type 2 diabetes.

1 was initially isolated as a lysine salt of the active pharmaceutical ingredient (API). However, the material was found to be poorly crystalline via X-ray powder diffraction (XRPD), and the differential scanning calorimeter (DSC) curve was complicated due to multiple thermal events. Further investigations indicated that the lysine salt was very hygroscopic above 65% relative humidity and difficult to scale up due to the high volume of solvent required (>100 vol. EtOH) for crystallization of the desired form. For these reasons, the free acid of **1** was investigated as a potential form for development with improved physical characteristics over the lysine salt. The

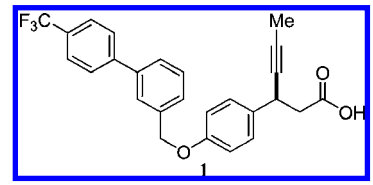

Figure 1. **Chemical structure of AMG 837.**

XRPD pattern of the free acid indicated that the material was crystalline; however, the DSC curve revealed that the form had a low onset of melting around 80 °C. A benchtop polymorph screen was conducted on the free acid to determine if there were any higher melting polymorphs, but no new phases were identified. Samples of the free acid were typically produced as thick oils that were slow to crystallize (days), and recrystallization was difficult due to the surfactant-like nature of the molecule. The free acid was also poorly soluble (∼0.5 mg/mL in water) and had poor wettability and poor solution- and solid-state stability, and required purification via salt formation.

The formation of crystalline salts is an approach used for optimization of physical properties such as melting point, hygroscopicity, chemical stability, dissolution rate, and crystal form.[9−14] Due to the unsuitable nature of the lysine salt and free acid forms of **1**, a full salt-screening investigation was conducted in order to identify a crystalline form with acceptable physical characteristics suitable for development.

2. Results and Discussion

2.1. Salt Screen. A salt screen was conducted using a variety of counterions including sodium, potassium, calcium, magnesium, ethanolamine, tris(hydroxymethyl)aminomethane (TRIS), choline, meglumine, L-histidine, and L-arginine. Four crystalline hits were identified and are summarized in Figures 2 and 3.

The potassium, magnesium, and anhydrous calcium salts were deprioritized because they yielded amorphous powders. The ethanolamine salt was deprioritized since no marketed oral drugs containing ethanolamine as a counterion were identified.[15] Although toxicology data from marketed (short duration use)

* To whom correspondence should be sent. E-mail: hmorriso@amgen.com. Telephone: 805-313-5502. Fax: 805-498-8674.

(1) Woo, J. C. S.; Cui, S.; Walker, S. D.; Faul, M. M. *Tetrahedron* **2010**, *66*, 4730–4737.
(2) Xie, Y.; Tao, W.; Morrison, H.; Chiu, R.; Jona, J.; Fang, J.; Couchon, N. *J. Pharm. Sci.* **2008**, *362*, 29–36.
(3) Briscoe, C. P.; Peat, A. J.; McKeown, S. C.; Corbett, D. F.; Goetz, A. S.; Littleton, T. R.; McCoy, D. C.; Kenakin, T. P.; Andrews, J. L.; Ammala, C.; Fornwald, J. A.; Ignar, D. M.; Jenkinson, S. *Br. J. Pharmacol.* **2006**, *148*, 619–628.
(4) Itoh, Y.; Hinuma, S. *Hepatol.Res.* **2005**, *33*, 171–173.
(5) Feng, D. D.; Luo, Z.; Roh, S. G.; Hernandez, M.; Tawadros, N.; Keating, D. J.; Chen, C. *Endocrinology.* **2006**, *147*, 674–682.
(6) Fujiwara, K.; Maekawa, F.; Yada, T. *Am.J.Physiol.Endocrinol.Metab.* **2005**, *289*, E670−677.
(7) Schnell, S.; Schaefer, M.; Schofl, C. *Mol. Cell. Endocrinol.* **2007**, *263*, 173–180.
(8) Song, F.; Lu, S.; Gunnet, J.; Xu, J. Z.; Wines, P.; Proost, J.; Liang, Y.; Baumann, C.; Lenhard, J.; Murray, W. V.; Demarest, K. T.; Kuo, G. H. *J. Med. Chem.* **2007**, *50*, 2807–2817.
(9) Gould, P. L. *Int. J. Pharm.* **1986**, *33*, 201–217.
(10) Bastin, R. J.; Bowker, M. J.; Slater, B. *J. Org Process Res Dev.* **2000**, *4*, 427–435.
(11) Stahl, P. H., Wermuth, C. G. *Handbook of Pharmaceutical Salts: Properties, Selection and Use*; Helvetica Chimica Acta: Zurich, 2002.
(12) Gross, T. D.; Schaab, K.; Ouellette, M.; Zook, S.; Reddy, J. P.; Shurtleff, A.; Sacaan, A. I.; Aebic-Kolbah, T.; Bozigian, H. *Org.Process Res.Dev.* **2007**, *11*, 365–377.
(13) Maurin, M. B.; Rowe, S. M.; Koval, C. A.; Hussain, M. A. *J. Pharm. Sci.* **1994**, *83* (10), 1418–1420.
(14) Kumar, L.; Amin, A.; Bansal, A. K. *Pharm.Technol.* **2008**, *3* (32), 128–146.
(15) For a GMP scale-up of an ethanolamine salt, see: Deussen, H.-J.; Jeppesen, L.; Scharer, N.; Junager, F.; Bentzen, B.; Weber, B.; Weil, V.; Mozer, S. J.; Sauerberg, P. *Org. Process Res. Dev.* **2004**, *8*, 363.

Published on Web 11/30/2010

10.1021/op100204u

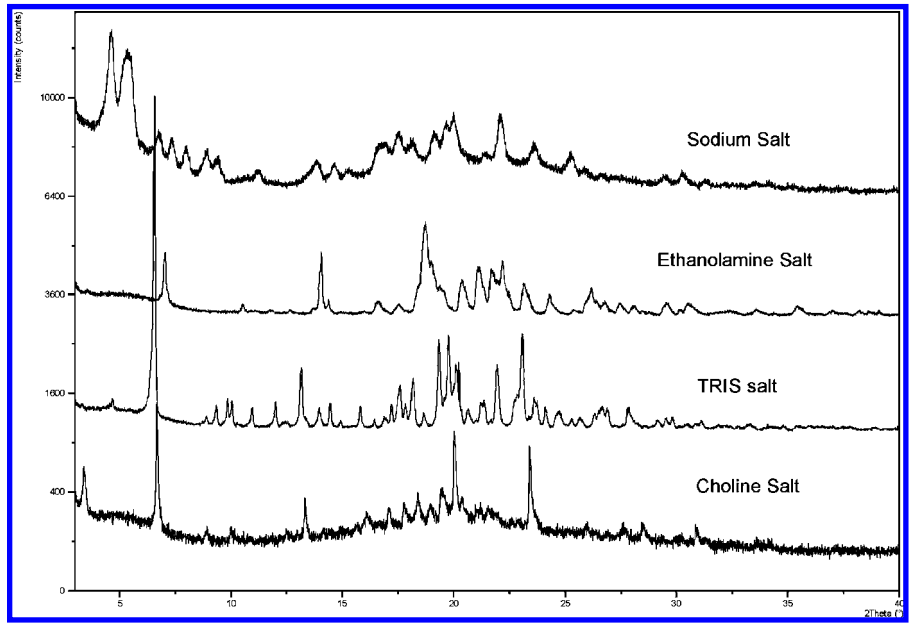

Figure 2. **Summary of XRPD patterns for crystalline salts.**

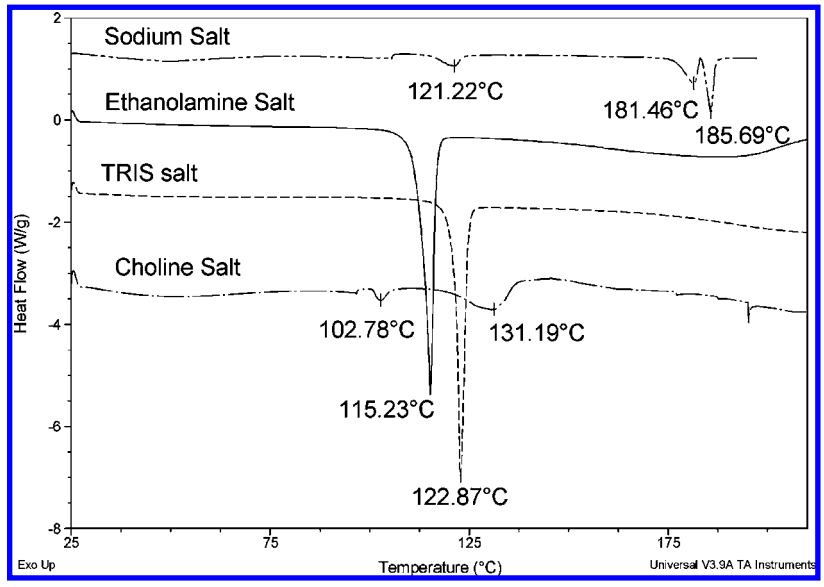

Figure 3. **Summary of DSC curves for crystalline salts.**

oral NSAID and antibiotic TRIS salts were favorable, this counterion had not been employed in an oral drug for chronic use at the time of this work. Consequently, although the TRIS salt was a viable pharmaceutical form, it was considered a second-tier choice relative to the more commonly employed and widely accepted inorganic counterions. The remaining leads were the sodium and choline salts, which were both lower crystalline salts, with DSC curves having multiple thermal events. The sodium salt was pursued for reasons outlined above and because it had a higher melt than the choline salt.

2.2. Polymorph Screen of the Sodium Salt. A full polymorph screen was conducted on the sodium salt (Figures 4 and 5). All phases yielded an XRPD pattern characterized by broad reflections and an underlying amorphous halo, except forms E and H. On the basis of XRPD data, form E was the first phase investigated. Thermal and vapor sorption analysis indicated that form E was an acetonitrile solvate and was not further developed due to the high levels of residual solvent present (monosolvate: 8 wt % MeCN) and because at ambient relative humidity conditions, it converted into a hemihydrate (form C). Desolvation of form E via heating past the desolvation event yielded form H, an unsolvated phase. Form G was also an unsolvated phase (highest melting phase at 184−187 °C), and therefore forms G and H were examined in more detail. Vapor sorption analysis indicated that, like the acetonitrile solvate, at ambient relative humidity conditions they both converted to the hemihydrate. Consequently, the hemihydrate (Form C) was the most yielded pattern from the various crystallization experiments of the benchtop polymorph screen. In addition, form C was found to have a water solubility greater than 100 mg/mL which was a significant improvement over the free acid form of **1**. Therefore, form C of the sodium salt was selected as the phase of interest and was investigated further.

The sodium salt of **1** was successfully scaled up for good laboratory practice (GLP) use by first crystallizing and isolating the acetonitrile-solvate (form E) from aqueous MeCN and then

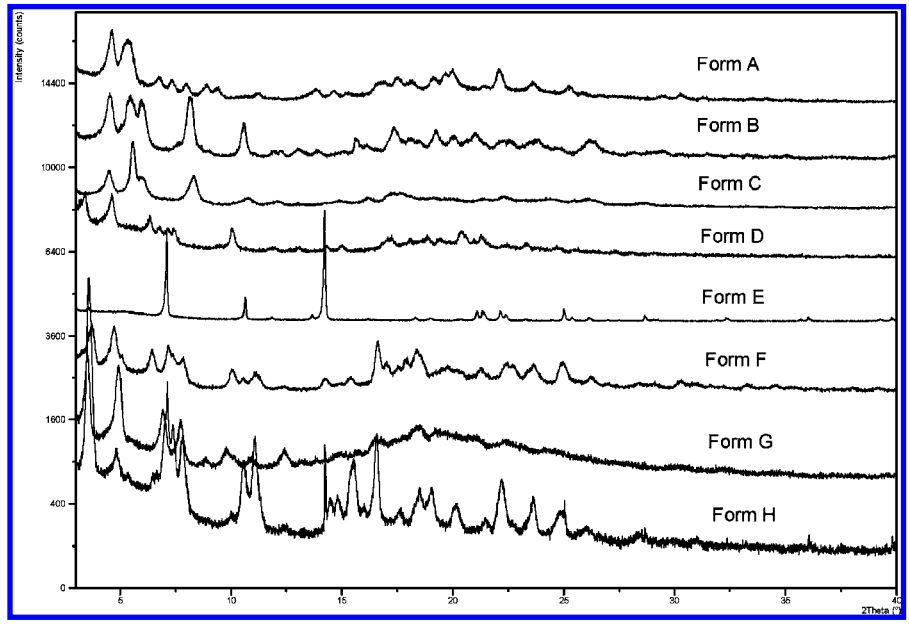

Figure 4. **Summary of XRPD patterns from the sodium salt polymorph screen.**

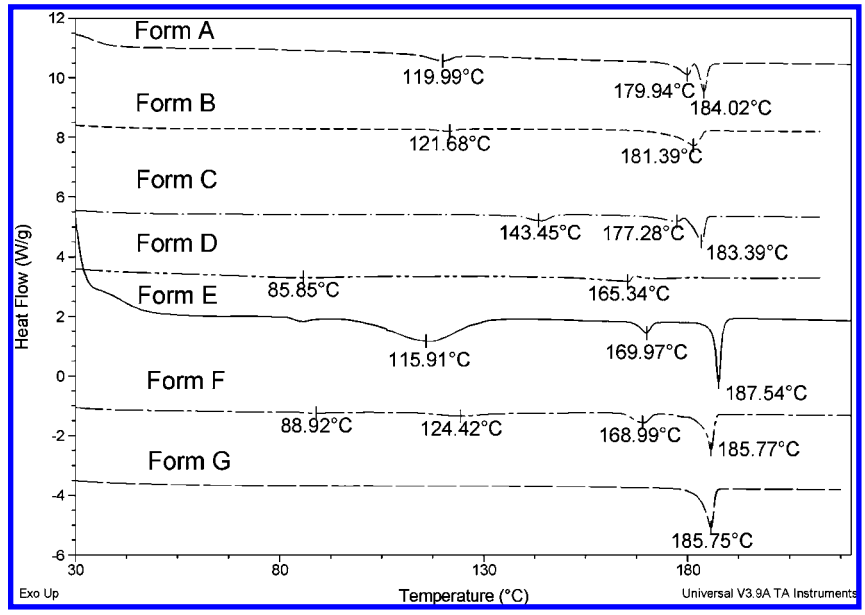

Figure 5. **Summary of DSC curves from the sodium salt polymorph screen.**

desolvating this material to the target form C. The XRPD, DSC and dynamic vapor sorption data are shown in Figures 6−8. The material was found to be low crystalline via XRPD and the other physical characterization data were in good agreement with data on the form C material isolated during the polymorph screen. Form C material was later scaled up further as a good manufacturing (GMP) lot using the same conditions as the previous lot (Figures 6−8). The crystallinity and hygroscopicity profile showed improvement in the GMP lot, when compared to the physical characterization data of the GLP lot, on the basis of the XRPD and moisture balance data.[16] The XRPD pattern shows stronger and more defined reflections (improved crystallinity), while light microscopy indicated 100 μm plate like crystals. The hygroscopicity profile shows stability up to 65% relative humidity compared to the 55% relative humidity limit of the GLP lot. The GMP lot was also found to be highly hygroscopic above 65% RH (33% weight change at 95% RH); however, the final material isolated from the post-run moisture balance experiment showed no form change when examined by XRPD, even though the post-run material showed a weight gain of 5% over the original starting material.

Upon successfully having scaled up a GMP lot of form C, it was important to fully understand the various thermal events seen in the DSC curve. As shown in Figure 7, there are 4 thermal events in the DSC curve. A broad endotherm around 61 °C, two sharper endotherms around 151 and 182 °C, and a major endotherm around 187 °C attributed to the melt of form G. A sample of the GMP lot (form C) was loaded onto the variable temperature XRPD instrument and heated just past each

(16) Slightly improved crystallinity in the GMP batch was attributed to improved control of the desolvation (Form E → Form C) process that employed a humid nitrogen sweep through the filter cake to induce the conversion.

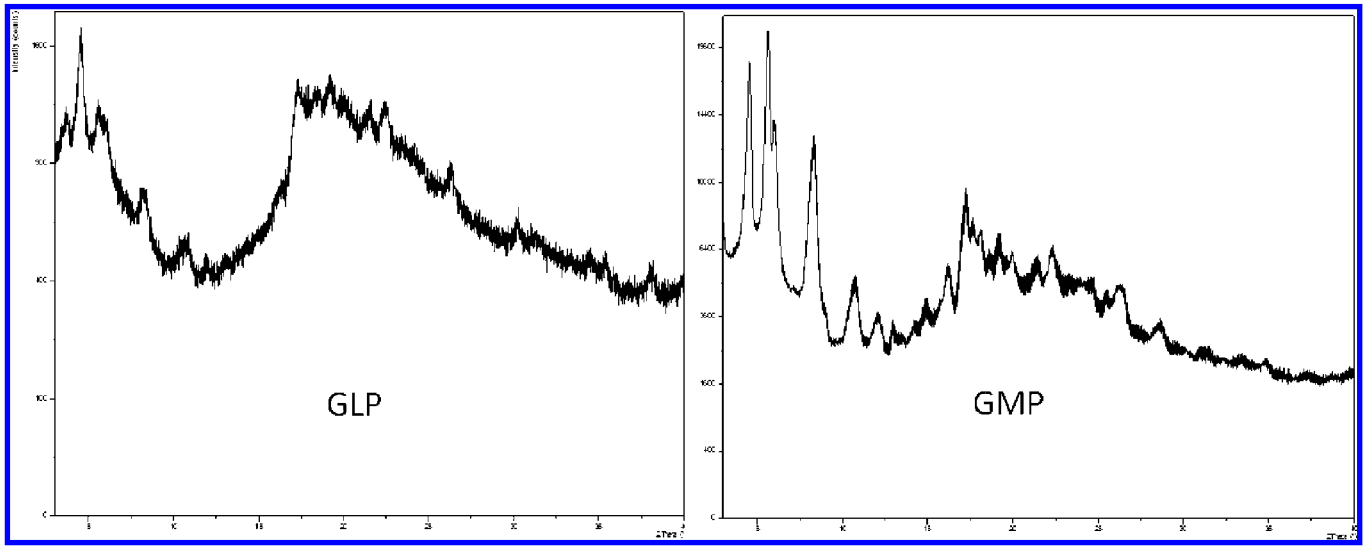

Figure 6. **XRPD for the sodium salt, GLP and GMP lots, form C.**

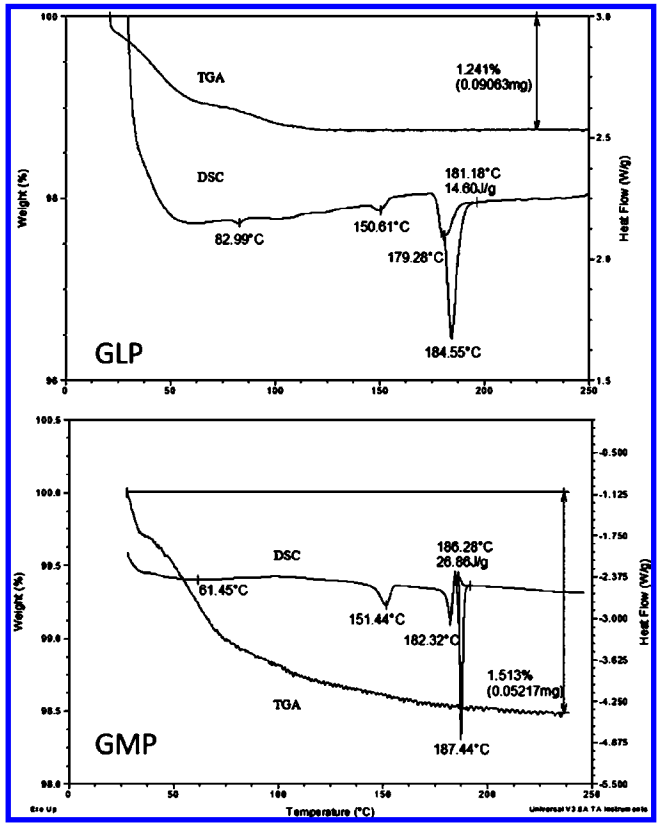

Figure 7. **DSC and TGA curves for the sodium salt, GLP and GMP lots, form C.**

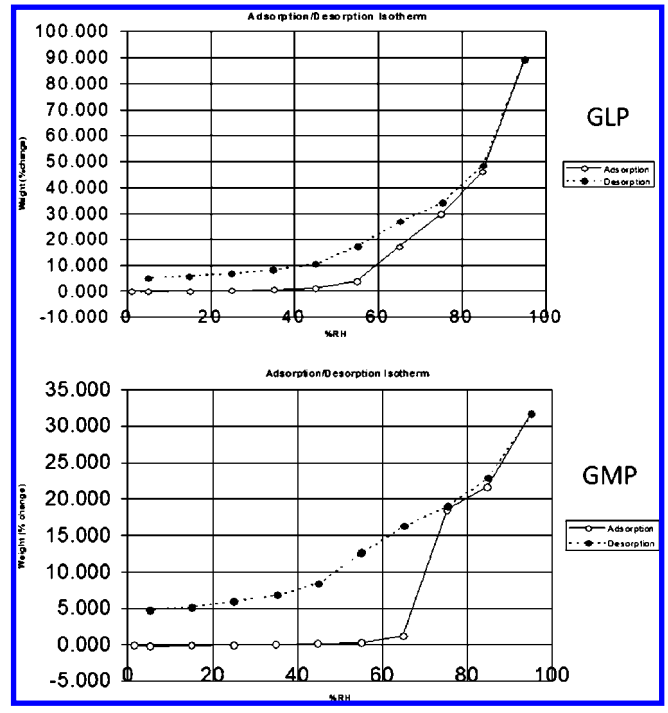

Figure 8. **Moisture balance curves for the sodium salt, GLP and GMP lots, form C.**

of the first three thermal events and characterized (Figure 9). When the material was heated to 120 °C (past the desolvation temperature seen in the TG) the sample only underwent very slight changes in the XRPD pattern, attributed to a conversion to an isomorphous dehydrated hydrate. When the sample was further heated beyond the second thermal event to 165 °C, a new form was identified via XRPD (form I) which did not match any of the previously characterized phases. Finally, when the sample was further heated beyond the third thermal event to 183 °C, XRPD data indicated the material had converted to form G, which is the highest melting unsolvated phase.

In order to determine if a low crystalline, highly hygroscopic phase can be suitable for development, several stress experiments were set up to investigate the physical stability of form C. These experiments were designed to determine if the form could endure the stress of formulation into drug product. To assay the effect of humidity, a portion of the GMP batch was stored in an open container at 68% relative humidity for 2 days. The XRPD and TG data for the post stressed sample were in very good agreement with that of the starting material. Due to concerns that Form C material might desolvate and change form during the drug product formulation process, portions of the GLP drug substance batch were stored in open vials at 60 °C/26%RH and 60 °C/50%RH for three hours. The XRPD and TG data for the post stressed samples were in very good agreement with that of the starting material. This data suggested

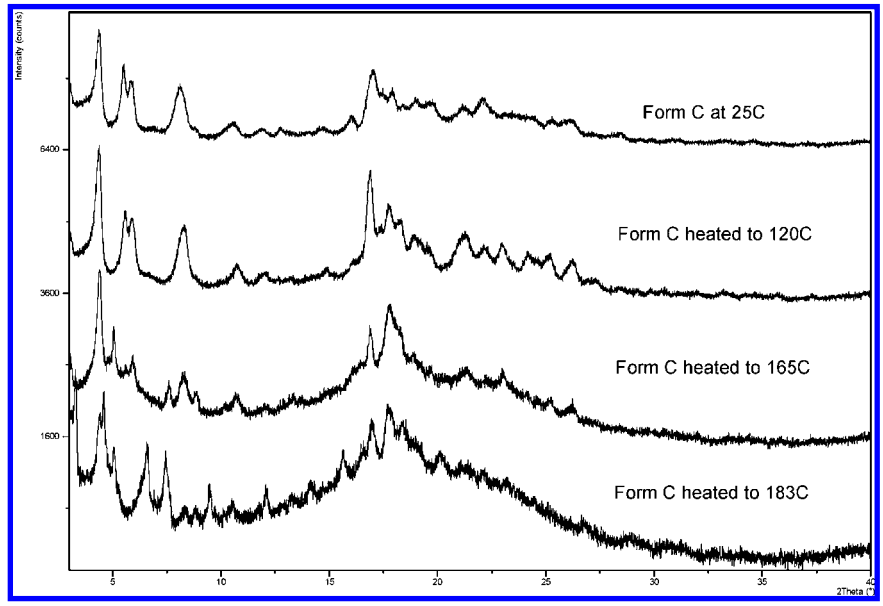

Figure 9. **Variable-temperature XRPD data on the sodium salt, form C.**

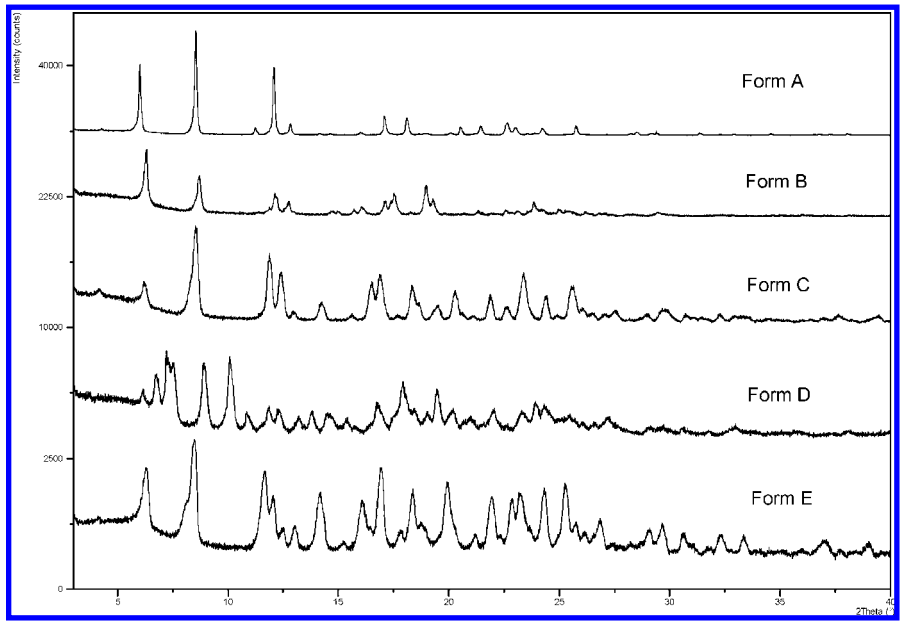

Figure 10. **Summary of XRPD patterns from the calcium salt polymorph screen.**

that the API form should be stable through the drying and tablet compression processes required for tablet formulation.

On the basis of all of the data collected on the sodium salt, it was decided that form C would be a suitable form for phase I clinical investigations, but not for long-term development (low crystallinity, complicated DSC profile, hygroscopic). Therefore, work was done to further examine some of the salt candidates that appeared amorphous from the salt screen, specifically the calcium salt. Previous attempts to isolate a calcium salt through reaction of the aqueous calcium counterion directly with the API in organic solutions yielded amorphous powders. A new approach to generate a crystalline calcium salt was investigated where the sodium salt of **1** was dissolved in water and the solution was charged with calcium chloride to induce precipitation of a calcium salt. This experiment yielded a crystalline calcium salt which was then scaled up for complete characterization and polymorph screening.

2.3. Polymorph Screen of the Calcium Salt. A full polymorph screen was conducted using both amorphous and the new crystalline calcium salt as starting material, and the results are shown in Figures 10 and 11. Several crystalline phases where characterized via XRPD, DSC, TG and dynamic moisture sorption and designated forms A-E. Form A was determined to be a methanolate, forms B and C were dihydrates, Form D was an isopropanol solvate, and form E was a pentahydrate. Further investigations were conducted on the two dihydrates (forms B and C) because the MeOH and IPA solvates were not of interest due to residual solvent levels, and the pentahydrate (form E) was shown to convert to form C when stressed by mild heating or exposure to less than 55% relative humidity. Further characterization indicated that none of the crystalline phases exhibited a true melt. In each case, the endotherm in the DSC curve for each phase was due to a desolvation event which yielded an amorphous phase post

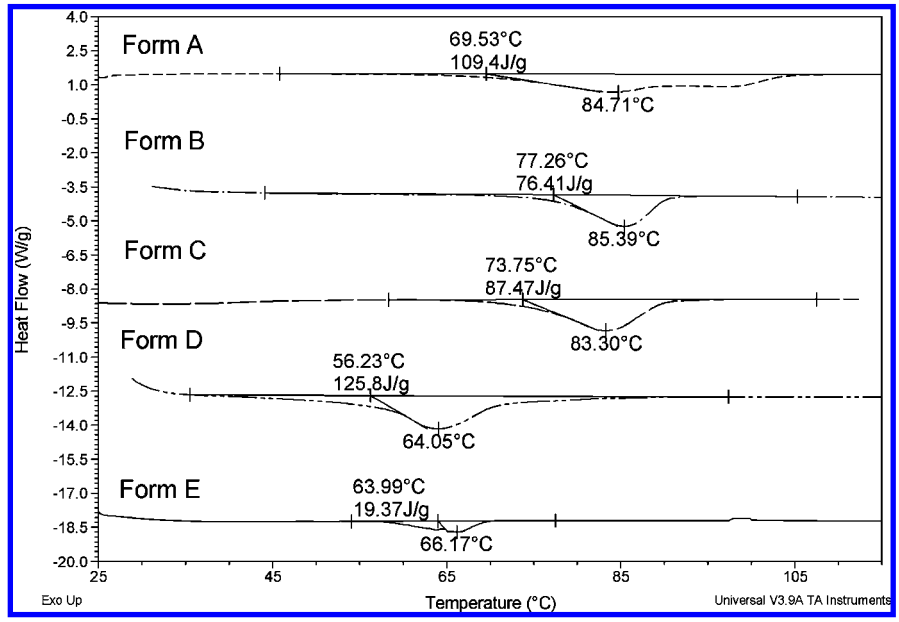

Figure 11. **Summary of DSC curves from the calcium salt polymorph screen.**

Table 1. **Summary of calcium salt forms B and C and amorphous solubilities in water**

starting phase	temperature of water (°C)	av solubility (mg/mL)[a]	resulting phase	av pH of resulting slurry[a]
B	5	0.002	B	8.2
B	21	0.001	B	8.3
B	40	0.001	B	8.7
C	5	0.068	C	9.2
C	21	0.062	C	9.1
C	40	0.003	amorphous + C	9.0
amorphous	5	0.001	amorphous	8.3
amorphous	21	0.003	amorphous	8.5
amorphous	40	0.001	amorphous	8.7

[a] $N = 3$, average of three measurements.

heating with a glass transition determined to be ~58 °C. This indicated that the crystalline phases required a guest solvent molecule to stabilize the crystal lattice.

Since forms B and C are both dihydrates, they are true polymorphs. To understand the relationship between these two dihydrates, the solubility of forms B, C and amorphous calcium salt were measured in water at three different temperatures (5, 21, and 40 °C). The results are summarized in Table 1. The data indicate that at all three temperatures, form B and the amorphous phase have a lower solubility in water than form C. The solubility of form C at 40 °C is significantly lower than at 5 and 21 °C and is attributed to the phase change that occurs during the experiment (resulting solids partially converted to an amorphous phase). It is rare to see an amorphous phase have a lower solubility than a crystalline hydrate, but this seemingly strange observation was attributed to the poor wettability of the amorphous phase compared to those of forms B and C. Since form B was shown to have lower solubility than form C at multiple temperatures in water, this indicated that at these temperatures form B was the thermodynamically stable hydrated phase and was selected as the phase of interest for the calcium salt.

Several stress experiments were set up to investigate the physical stability of form B. The moisture balance curve for

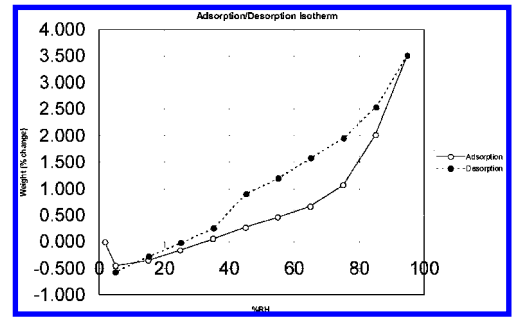

Figure 12. **Moisture balance curve for the calcium salt, form B.**

form B is shown in Figure 12 and indicates that the calcium salt is far less hygroscopic (3.5% weight change at 95% RH) than the previously characterized sodium salt. Although superior crystallinity and hygroscopicity of the calcium salt are an advantage over those of the sodium salt, there was concern that the calcium salt form B material might undergo a phase change to amorphous during the process of formulating the drug product. Therefore, material was heated at various relative humidities to mimic the stress of drug product formulation. When form B material was stressed at either 40 or 40 °C/75% RH up to 4 weeks, the phase remained unchanged, while form B material stored at 60 °C for 12 days became amorphous. When form B material was stressed at 70 °C/5% RH, the material began to show signs of an amorphous halo via XRPD after 20 min of exposure, while form B material stressed at 70 °C/11% RH and 70 °C/24% RH began to show signs of an amorphous halo via XRPD after 30 min of exposure. This data indicated that drug product drying conditions were critical and should be close to 40 °C. To mimic the conditions of a wet granulation process, form B was subjected to small scale wet milling conditions to determine if conversion to amorphous would occur under forcing conditions. Thus, 30 mg of the salt in 1.5 mL of water was milled with a stainless steel ball for three minutes. XRPD analysis before and after milling indicated no change in form and that the milled material had not lost

Table 2. **Comparison of the sodium salt form C and calcium salt form B**

	sodium salt	calcium salt
hygroscopicity	hygroscopic	nonhygroscopic
crystallinity	poorly crystalline	crystalline
API stability	must be stored under refrigerated conditions and protected from light and humidity, and ambient humidity must be controlled on handling	stable ≥3 months at 40 °C/75% RH without desiccant
API manufacture	scalable	scalable, requires drying below 40 °C to avoid erosion of crystallinity due to dehydration
tablet manufacture	challenging to use wet granulation due to content uniformity concerns	feasible to use either wet granulation or dry process
solubility	high aqueous solubility (>100 mg/mL)	low aqueous solubility (0.003 mg/mL)
PK data	sodium salt solution and a calcium salt suspension (1 mg/kg dose) have a PK/BA profile similar to that in monkey	

crystallinity. This suggested that form B of the calcium salt would maintain its physical stability though a wet granulation.

After reinvestigating the calcium salt and identifying several crystalline phases, form B was found to be a potentially viable form for future development along with form C of the sodium salt. The two salts were therefore compared on the basis of several criteria to determine which phase represented the best path forward.

2.4. Final Salt Form Selection. In order to determine which salt (sodium or calcium) should be recommended for product development, the following quality attributes were compared: hygroscopicity, crystallinity, API stability, API scale up, drug product (tablet) manufacturability, solubility, and PK exposure. The data are summarized in Table 2. The calcium salt was found to be a crystalline phase that is nonhygroscopic while the sodium salt was poorly crystalline and very hygroscopic above 65% RH. With respect to API stability, the calcium salt was found to be stable up to 3 months at 40 °C/75% RH without desiccation, whereas the sodium salt required storage at 2−8 °C, required protection from light and humidity and required control of ambient humidity on handling. Manufacture of both salts was scalable and although the calcium salt had a low phase transition (∼58 °C), suitable conditions were developed to dry (<40 °C) the material without causing erosion of crystallinity due to dehydration. It was feasible to use either wet granulation or a dry process for the calcium salt for tablet manufacture, while it would be very challenging to use wet granulation for the sodium salt due to content uniformity issues arising from the high water solubility. This was a concern for low strength drug (<1 mg) formulations, where wet granulation is commonly used. The calcium salt had significantly lower aqueous solubility (0.003 mg/mL) than the sodium salt (>100 mg/mL), and thus a pharmacokinetics (PK) study in nonhuman primates was conducted to compare bioavailability (BA) after oral dosage of the two salts. The data indicated that a sodium salt solution and a calcium salt suspension at 1 mg/kg level had a similar PK/BA profile in nonhuman primates; thus, exposure was not solubility limited.

In summary, due to the superior properties of the calcium salt (form B) relative to the sodium salt (form C), the calcium salt was recommended for product development.

3. Materials and Methods

3.1. Materials. 1 was manufactured by the Process Research and Development division of Amgen Inc., Thousand Oaks, CA. All water used was distilled twice and deionized. All other reagents were analytical grades unless otherwise stated.

4. Experimental Section

4.1. X-ray Powder Diffraction (XRPD). X-ray powder diffraction (XRPD) patterns were collected using a Phillips X-ray automated powder diffractometer (X'Pert). Diffraction patterns were collected at room temperature between 3−40 degree 2-Theta with a step size of 0.008 degrees and a counting time of 15.24 s. Instrument voltage was 45 kV while the current was 40 mA. Variable temperature XRPD patterns were collected with a heating stage chamber accessory using the instrumental parameters described above.

4.2. Differential Scanning Calorimetry (DSC). A portion of each powder sample (<1−5 mg) was loaded into crimped or open aluminum DSC pans and characterized on either a TA Instruments DSC 2920, Q 100 or Q 1000. Data analysis was performed utilizing Universal Analysis 2000, TA Instruments. A heating rate of 10 °C/min was used over a variety of temperature ranges.

4.3. Thermogravimetric Analysis (TGA). Thermogravimetric analysis was performed on samples using a TA Instruments TGA 2950 or Q 500. A heating rate of 10 °C/min was used over a variety of temperature ranges. Data analysis was performed utilizing Universal Analysis 2000, TA Instruments.

4.4. Dynamic Vapor Sorption Analysis. Dynamic vapor sorption data were collected using a VTI SGA 100 symmetrical vapor sorption analyzer. Relative humidity was varied in increments of 5%, starting at 5% relative humidity thereby increasing to 95% relative humidity, and then undergoing a drying cycle back to 5% relative humidity. Equilibrium criteria were set at 0.01% weight change in 1 min with a maximum equilibrium time of 180 min. Approximately 1−15 mg of sample was used.

4.5. Polymorph and Salt Screening. Recrystallization experiments included evaporation, slurries, antisolvent addition, vapor diffusion chambers and heating experiments. Evaporation experiments were conducted by dissolving a portion of the API in a given solvent, filtering the solution with a 0.45 μm PTFE filter into a vial, then either leaving the vial uncovered or covering the vial with pin-holed Parafilm. Slurry experiments were performed by saturating a giving solvent with API, such that excess solid was in constant contact with solution. The sample was then agitated on a slurry wheel at room temperature for approximately one week. Antisolvent addition experiments

were performed by dissolving a portion of the API in 1 mL of solvent followed by addition of 25 mL of antisolvent, and then cooling the solution in a refrigerator. Vapor diffusion chambers were generated by dissolving a portion of the API in a given solvent, filtering the solution with a 0.45 μm PTFE filter into a 3 mL vial, then placing that 3 mL vial inside of a scintillation vial containing several milliliters of antisolvent. The scintillation vial was then capped and allowed to sit for approximately one week.

4.6. High Performance Liquid Chromatography (HPLC). HPLC was run using an Agilent Series 1100 having a Phenomenex Luna C18 column (30 $\times$ 4.60 mm, 3 μm). Analyses were run with a gradient method using 98% water 2% acetonitrile (mobile phase A) and 98% acetonitrile 2% water (mobile phase B) with a gradient going from 10% to 95% B at a flow rate of 1 mL/min and a total run time of 5 min. UV detection was run at a wavelength of 254 nm.

4.7. Solubility Measurements. Solubility measurements were conducted by saturating a given solvent system with a test compound at a given temperature, and agitating the mixture for 24 h. The suspension was then filtered using a PTFE (0.45 μm) filter. The resulting solid phase was examined via XRPD, while the resulting solution was analyzed for drug concentration via HPLC.

5. Conclusions

A salt screening selection process was performed on AMG 837 (**1**) due to unfavorable physical characteristics (low melt, poor stability, poor water solubility) of the free acid form. Salts which were investigated included, sodium, meglumine, L-arginine, L-histidine, potassium, calcium, choline, magnesium, lysine, ethanolamine, and TRIS. Of those listed, the majority yielded amorphous or low crystalline material, while others were not preferred due to a lack of long-term (chronic) oral use data and its safety implication. The sodium and calcium salts were the only two to yield potentially viable phases. However, the sodium salt showed severe hygroscopicity above 65% RH while the calcium salt consisted of hydrates that dehydrate at a low temperature (~60−80 °C) and then become amorphous upon dehydration. Ultimately, a stable, crystalline hemicalcium salt dihydrate form was recommended for long-term product development.

Acknowledgment

We thank Shekman Wong, Leock Ngo, Sharon Baughman, Marintan Pandjaitan, Marie Du, Xiao Ding, and Maurice Emery for the supporting PK data for these investigations.

Supporting Information Available

Further experimental data. This material is available free of charge via the Internet at http://pubs.acs.org.

Received for review July 26, 2010.

OP100204U